nature methods

SUPPLEMENTARY INFORMATION

https://doi.org/10.1038/s41592-019-0688-0

In the format provided by the authors and unedited.

MINFLUX nanoscopy delivers 3D multicolor nanometer resolution in cells

Klaus C. Gwosch[1,4], Jasmin K. Pape[1,4], Francisco Balzarotti[1,4], Philipp Hoess[2], Jan Ellenberg[2], Jonas Ries[2] and Stefan W. Hell[1,3]*

[1]Department of NanoBiophotonics, Max Planck Institute for Biophysical Chemistry, Göttingen, Germany. [2]Cell Biology and Biophysics Unit, European Molecular Biology Laboratory (EMBL), Heidelberg, Germany. [3]Department of Optical Nanoscopy, Max Planck Institute for Medical Research, Heidelberg, Germany. [4]These authors contributed equally: Klaus C. Gwosch, Jasmin K. Pape, Francisco Balzarotti. *e-mail: stefan.hell@mpibpc.mpg.de

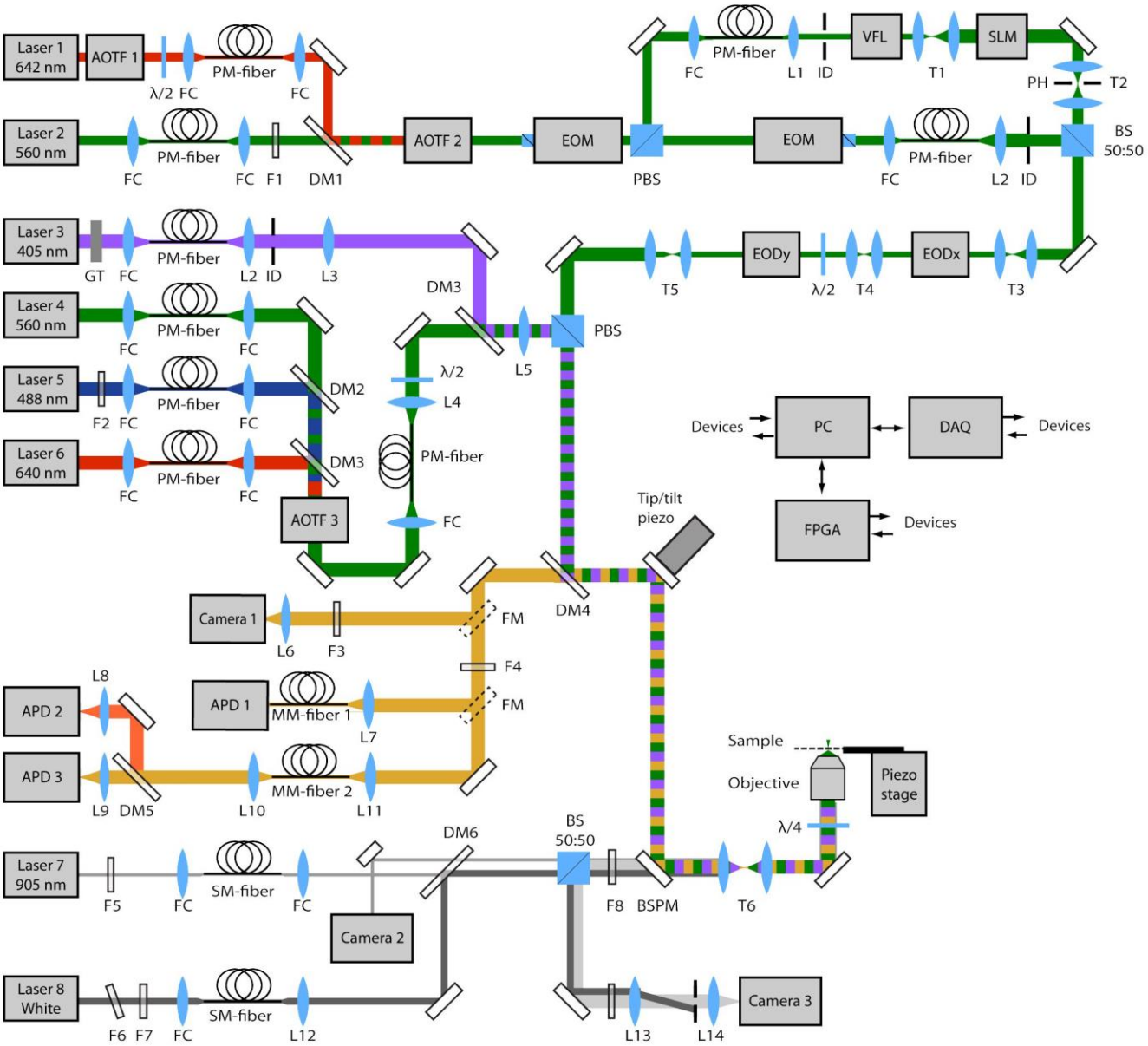

Supplementary Figure 1

Schematic drawing of the optical setup.

Lasers :
Laser 1: VFL-P-1500-642 (MPB Communications Inc., Pointe-Claire, Quebec, Canada),
Laser 2: Cobolt Jive™ 150-561 (Cobolt AB, Solna, Sweden),
Laser 3: 405-50-COL-004 (Oxxius, Lannion, France),
Laser 4: Cobolt Jive™ 25-561 (Cobolt AB, Solna, Sweden),
Laser 5: LDH-D-C-485 (PicoQuant, Berlin, Germany),
Laser 6: LDH-D-C-640 (PicoQuant, Berlin, Germany),
Laser 7: LuxX® 905-150 (Omicron-Laserage Laserproodukte GmbH, Rodgau-Dudenhofen, Germany),
Laser 8: Koheras SuperK Extreme (NKT Photonics, Birkerød, Denmark)

Beam modulation:
AOTF1: AOTFnC VIS-TN (AA Sa, Orsay, France),
AOTF2: AOTFnC VIS-TN (AA Sa, Orsay, France),
AOTF3: AOTFnC 400.650-TN (AA Sa, Orsay, France),
EOM: LM 0202 P 5W + LIV 20 (Qioptiq Photonics GmbH & Co. KG, Göttingen, Germany),
SLM: LCOS-SLM X13267-06 (Hamamatsu Photonics Deutschland GmbH, Herrsching am Ammersee, Germany),

Scanning:

EODx and EODy: M-311-A (Conoptics Inc., Danbury, CT, USA) + WMA-300 (Falco Systems BV, Amsterdam, The Netherlands),
VFL: KLMS2D0700 -00 KTN varifocal lens module (NTT Advanced Technology Corporation, Omiya-cho Saiwai-ku, Kawasaki-shi, Japan) + AMPS-2B200-03 (Matsusada Precision Inc., Aojicho Kusatsu, Japan),
Tip/tilt piezo: PSH-10/2 + EVD300 (both piezosystem jena GmbH, Jena, Germany),
Piezo stage: P-733.3-DD + E725 (both Physik Instrumente (PI) GmbH & Co. KG, Karlsruhe, Germany),

Polarization and beam transport:
GT: Glan-Thompson polarizer (B. Halle Nachfl. GmbH, Berlin, Germany),
PBS: polarizing beam splitter cube (B. Halle Nachfl. GmbH, Berlin, Germany),
BS: beam splitter cube 50:50,
FC: fiber collimator 60FC-* (Schäfter+Kirchhoff, Hamburg, Germany),
λ/2: half wave plate (B. Halle Nachfl. GmbH, Berlin, Germany or Thorlabs Inc., Newton, NJ, USA),
λ/4: achromatic quarter wave plate (Thorlabs Inc., Newton, NJ, USA),
PM-fiber: polarization maintaining single mode fiber (Thorlabs Inc., Newton, NJ, USA or Schäfter+Kirchhoff, Hamburg, Germany),
SM-fiber: single mode fiber (Thorlabs Inc., Newton, NJ, USA or Schäfter+Kirchhoff, Hamburg, Germany),
MM-fiber 1: multimode fiber M31L01 (Thorlabs Inc., Newton, NJ, USA),
MM-fiber 2: multimode fiber M42L02 (Thorlabs Inc., Newton, NJ, USA),

Lenses and mirrors
Objective: HC PL APO 100x/1.40 Oil CS2 (Leica Microsystems GmbH, Wetzlar, Germany),
L1-L14: achromatic lens with VIS or NIR AR coating (Thorlabs Inc., Newton, NJ, USA or Qioptiq Photonics GmbH & Co. KG, Göttingen, Germany),
T1-T6: telescope,
ID: iris diaphragm,
FM: mirror on motorized flip mount,
PH: pinhole,
BSPM: back side polished mirror (Thorlabs Inc., Newton, NJ, USA),

Dichroic mirrors and filters
DM1: H 568 LPXR superflat (AHF Analysetechnik GmbH, Tübingen, Germany),
DM2: Z500-RDC-XT (Chroma Technology Corp., Bellows Falls, VT, USA),
DM3: Z620SPRDC (Chroma Technology Corp., Bellows Falls, VT, USA),
DM4: ZT405/488/561/640rpc (AHF Analysetechnik GmbH, Tübingen, Germany),
DM5: FF685-Di02 (Semrock Inc., Rochester, NY, USA),
DM6: FF925-Di01 (Semrock Inc., Rochester, NY, USA),
F1: ZET561/10x (Chroma Technology Corp., Bellows Falls, VT, USA),
F2: 488/6 BrighLine HC (Semrock Inc., Rochester, NY, USA),
F3: FF01-842/SP-25 (Semrock Inc., Rochester, NY, USA) and Quad-Band 446/523/600/677 HC (Semrock Inc., Rochester, NY, USA),
F4: FF01-775/SP-25 (Semrock Inc., Rochester, NY, USA) and Quad-Notch 405/488/560/635 (Semrock Inc., Rochester, NY, USA) and ET700/75m (Chroma Technology Corp., Bellows Falls, VT, USA) or BLP02-561R-25 (Semrock Inc., Rochester, NY, USA),
F5: FL905/10 (Dynasil, Littleton, MA, USA),
F6: FELH0950 (Thorlabs Inc., Newton, NJ, USA),
F7: FESH1000 (Thorlabs Inc., Newton, NJ, USA),
F8: 66-230 long pass filter 950 (Edmund Optics®, Barrington, NJ; USA),

Detectors
APD 1: SPCM-AQR-13-FC (Excelitas Technologies, Waltham, MA, USA),
APD 2,3: SPCM-AQRH-13-TR (Excelitas Technologies, Waltham, MA, USA),
Camera 1: Ixon EMCCD DU897-BV, (Andor Technology Ltd., Belfast, UK),
Camera 2: DMK 22BUC03 (The Imaging Source Europe GmbH, Bremen, Germany),
Camera 3: DMK 23UP1300 (The Imaging Source Europe GmbH, Bremen, Germany),

Computer
PC: 3 personal computers running Windows 7 (Microsoft Corp., Redmond, WA, USA) and LabView 2016 (National Instruments, Austin, TX, USA),
DAQ: NI PCIe-6353 + NI PCI-6259 (both National Instruments, Austin, TX, USA) + USB-3133 (Measurement Computing Corporation, Norton, MA, USA),

FPGA: NI USB-7856R (National Instruments, Austin, TX, USA)

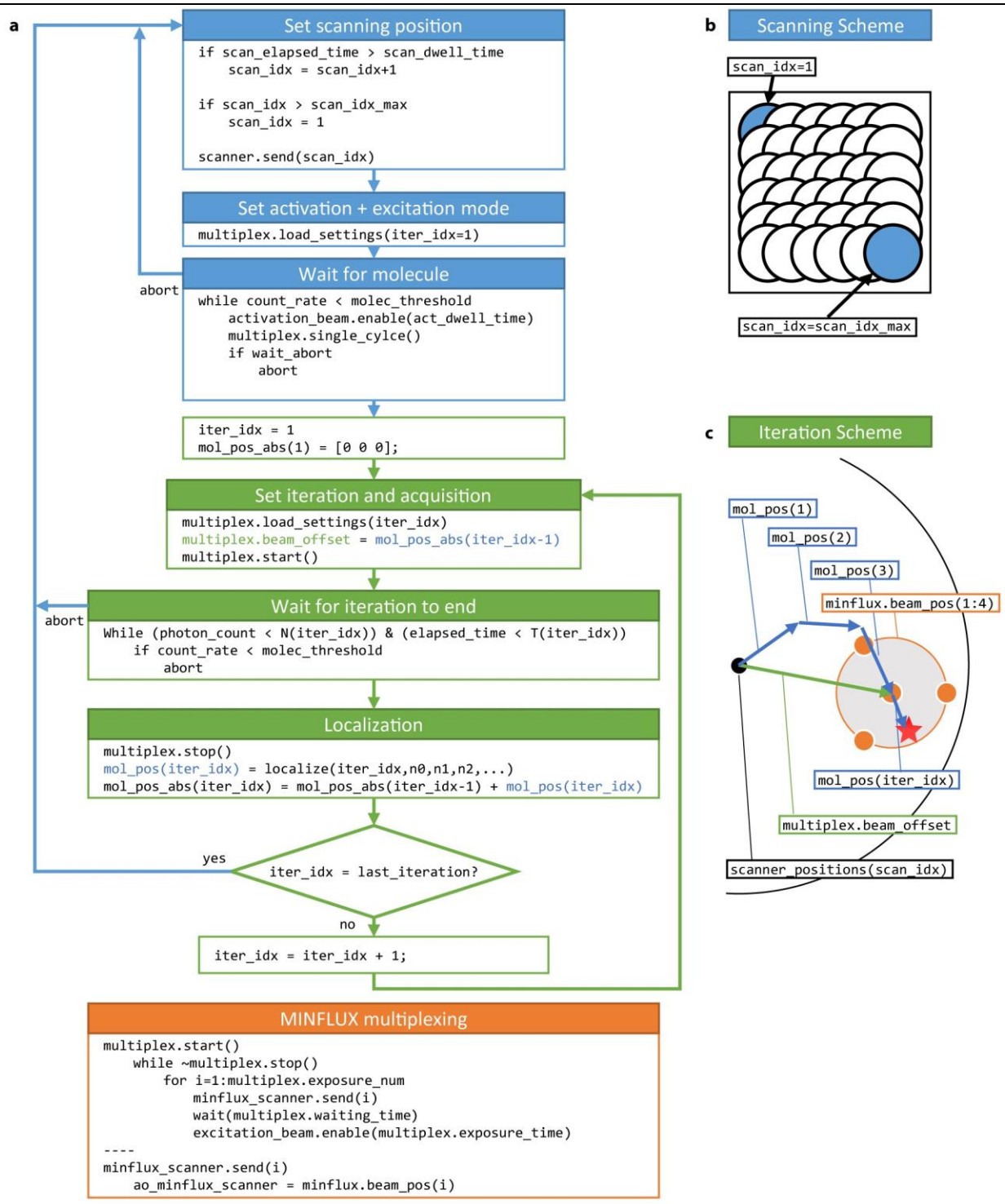

Supplementary Figure 2

Pseudo code for MINFLUX FPGA core.

a, Flowchart with pseudocode describing the FPGA core that controls the MINFLUX acquisition for imaging. The first part (blue) represents the control of the scanner that allows stitching a large image. The second part (green) represents the sequential MINFLUX iteration scheme. The third part (orange) represents the MINFLUX multiplexing for a given iteration. **b,** Representation of the scanning scheme. **c,** Representation of the iterative localizations produced for a single molecule (red star). The iteration scheme is represented at iteration `iter_idx = 4`. Each localization of the molecule (`mol_pos(1)`, `mol_pos(2)`, etc.) has a different frame of reference (`multiplex.beam_offset`), where the MINFLUX beam positions (`minflux.beam_pos`) are centered. Each final localization is obtained with respect to the main scanner frame of reference (`scanner_positions(scan_idx)`). A detailed reference for all variables and functions is provided in Tab. S1.

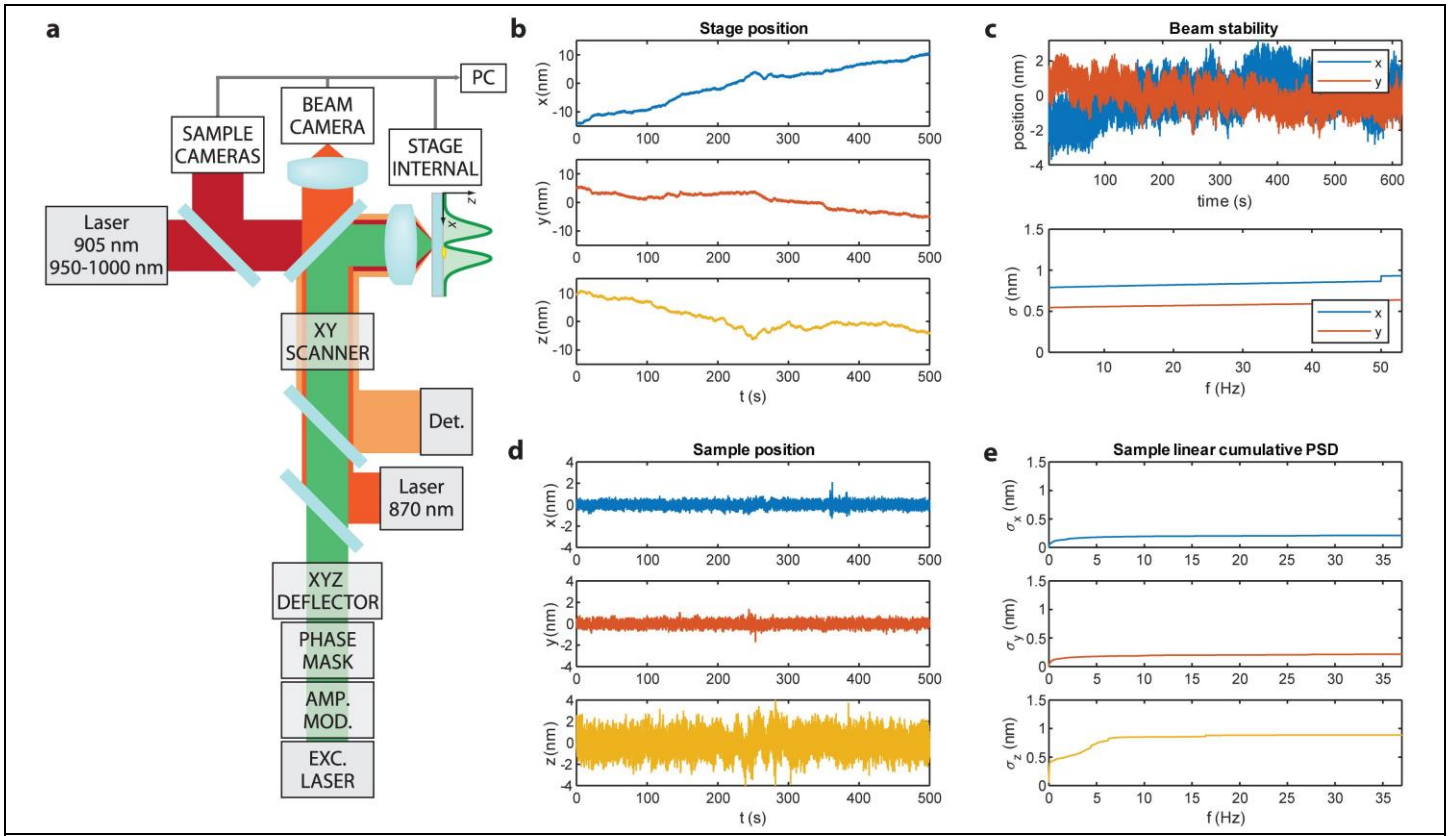

Supplementary Figure 3

Stability of the MINFLUX experiment.

a, Schematic of the stability measurement components. For measuring the sample position we used the stage lock system as described before and documented in Fig. S1 while monitoring the stage position using the internal position sensor of the piezo sample stage. We evaluated the beam stability by introducing an additional laser line of 870 nm, passing through a back-side polished mirror before the objective lens. We focused the beam onto a camera to evaluate the beam position using a Gaussian fit. All measurements are in units of displacements in the sample plane. **b**, Position of the stage when actively stabilizing the sample position (readout of the internal stage position sensors). **c**, Beam position (upper panel) and linear cumulative power-spectral density (PSD) (lower panel) taking into account drift of the optical components after the electro-optical parts of the setup. **d**, Actively stabilized sample position, measured using the position of a total internal reflection beam (*z*) and the position of fiducial markers on the sample plane (*xy*). **e**, Linear cumulative PSD of the stabilized sample position.

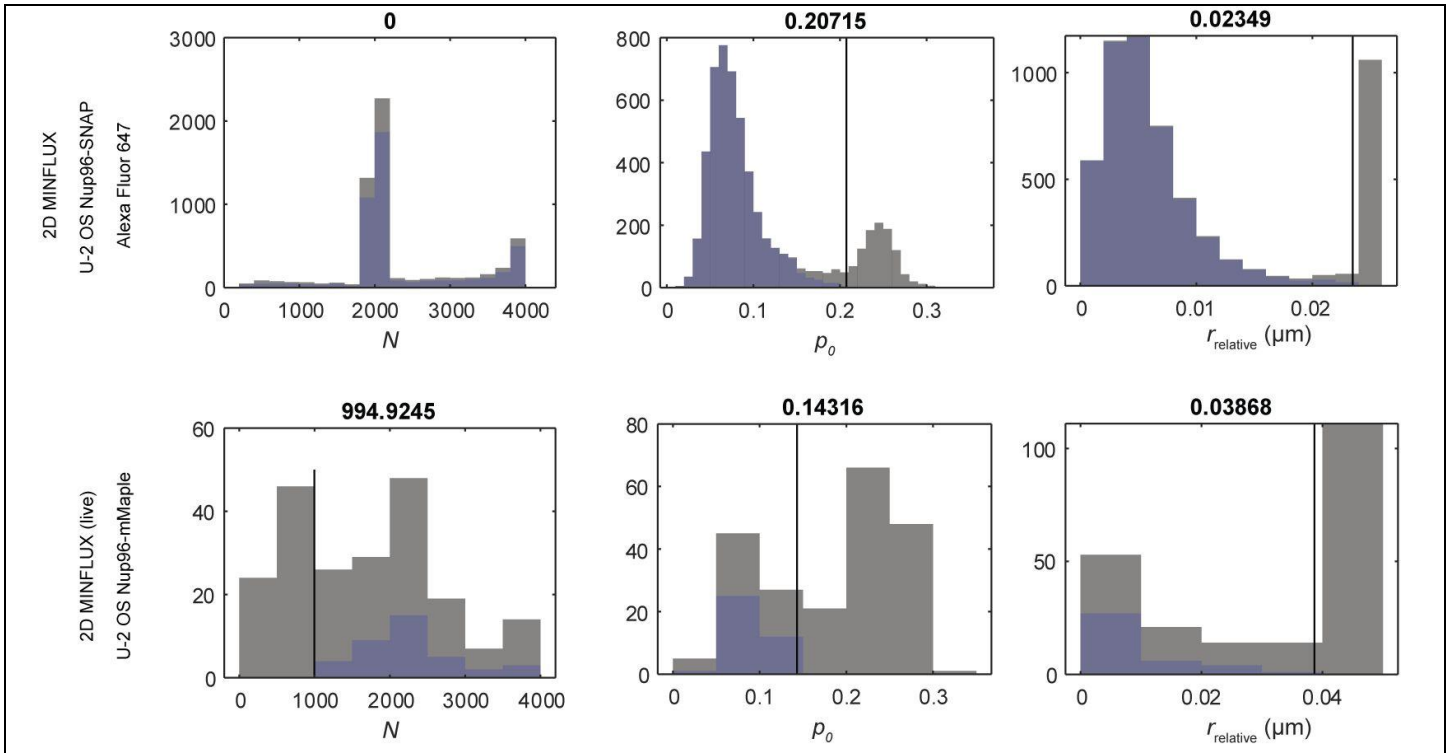

Supplementary Figure 4

Filtering of 2D imaging data.

The histogram of photon number *N*, the relative photon count number in the central exposure p_0 and distance of the estimated position relative to the center of the last excitation beam pattern $r_{relative}$ are displayed for each localization. Before filtering (gray) at a manually defined position (black line, number above), p_0 and $r_{relative}$ show two populations. The population that is assigned to background events is discarded, leading to a new filtered distribution (blue). Top row: data displayed in Fig. 2a. Bottom row: data displayed in Fig. 2f.

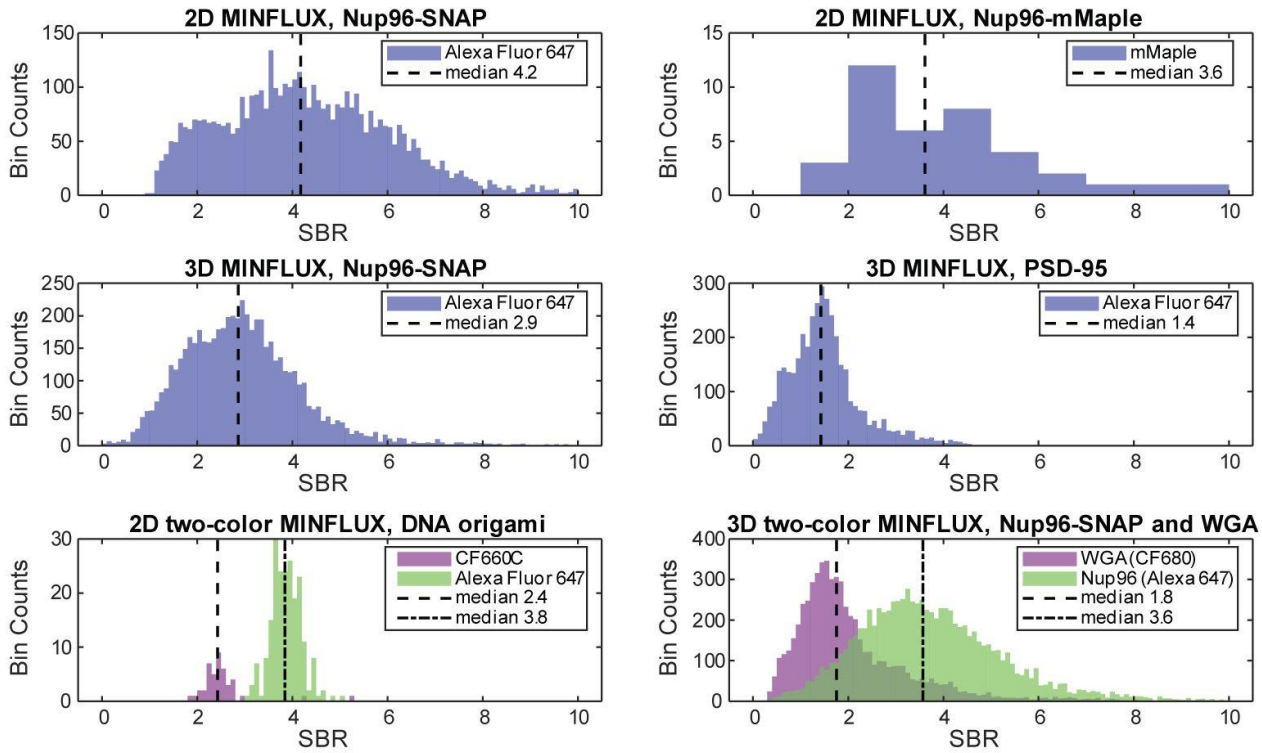

Supplementary Figure 5

Signal-to-background ratios in MINFLUX nanoscopy.

We estimated the signal-to-background-ratios (SBR) for all events from the switching-off step in the MINFLUX trace. We show an SBR histogram for each of the following datasets: 2D MINFLUX Nup96-SNAP (Fig. 2b), 2D MINFLUX NUP96-mMaple (Fig. 2f), 3D MINFLUX Nup96-SNAP (Fig. 3f), 3D MINFLUX PSD-95 (Fig. 4a), 2D two-color MINFLUX DNA origami (Fig. 5b) and 3D two-color MINFLUX Nup96-SNAP and WGA (Fig. 5c).

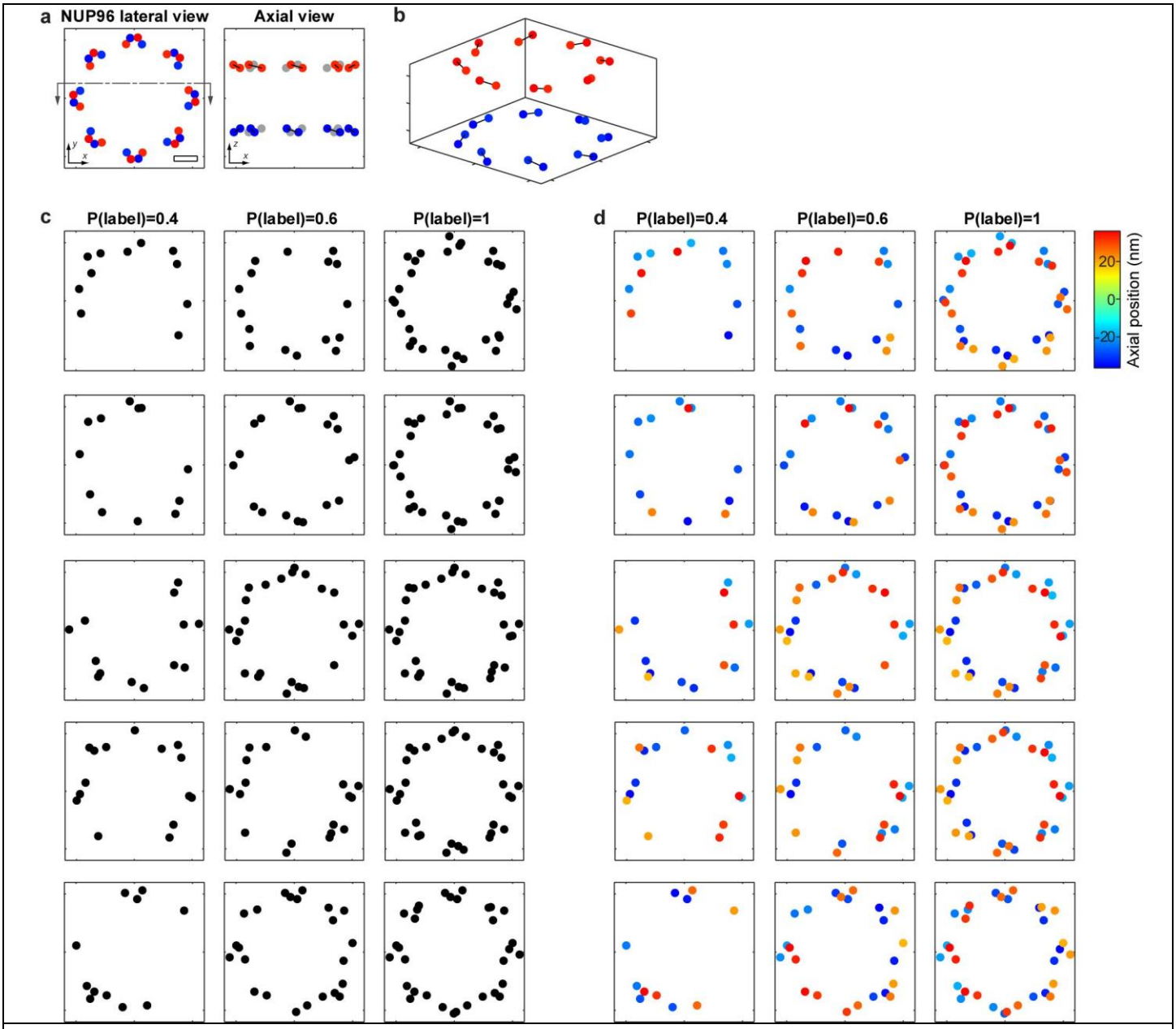

Supplementary Figure 6

Expected locations for NUP96.

a, Location of NUP96 subunits C termini, where the SNAP-tag was fused, we display the lateral (colors distinguish axial location) and axial views (dots behind the section line in the lateral view are grayed). **b**, Three dimensional view of the same structure. **c**, Simulations of the *xy* projection of the NUP96 C-termini location for different degrees of labeling (0.4, 0.6 and 1) with random rotations with respect to the *x* and *y* axes (uniform distribution, range 20 deg). Each row is the same rotation instance with different degrees of labeling. **d**, Identical to c, colored according to the axial location, with the intention of guiding the eye. Scale bar: (a) 20 nm, all other images have the same scale.

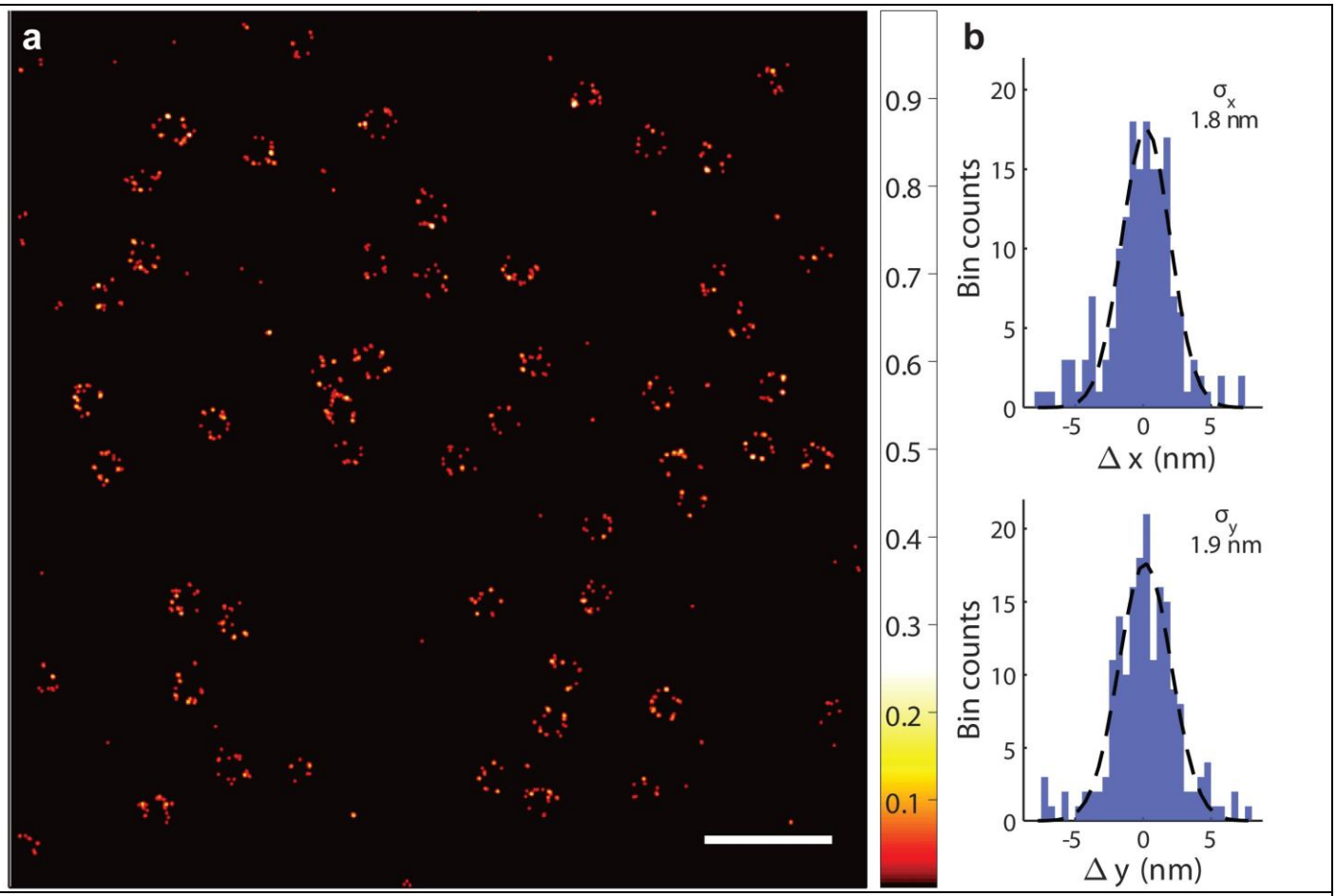

Supplementary Figure 7

MINFLUX nanoscopy of Nup96-mMaple in fixed cells.

a, Image of a fixed U-2 OS cell expressing the fusion protein Nup96-mMaple. Colorbar units: normalized to peak 2D histogram pixel; we shifted the colormap range to enhance visibility. **b**, 1D histograms of the distance from the individual localizations to the mean position of a single emitter. A Gaussian fit delivers 1D localization precisions around 2 nm in both directions. Scalebar: 500 nm.

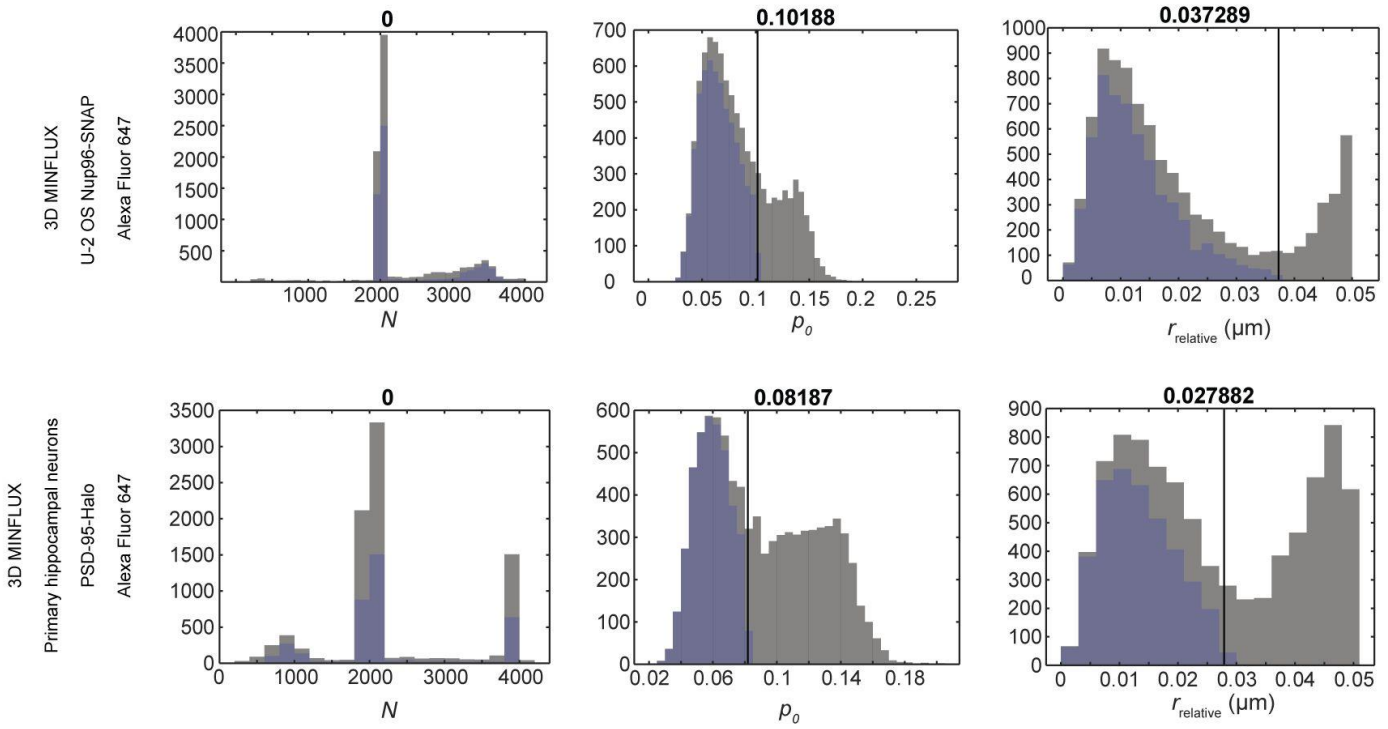

Supplementary Figure 8

Filtering of 3D imaging data.

The histogram of photon number *N*, the relative photon count number in the central exposure p_0 and distance of the estimated position relative to the center of the last excitation beam pattern $r_{relative}$ are displayed for each localization. Before filtering (gray) at a manually defined position (black line, number above), p_0 and $r_{relative}$ show two populations. The population that is assigned to background events is discarded, leading to a new filtered distribution (blue). Top row: data displayed in Fig. 3f. Bottom row: data displayed in Fig. 4a.

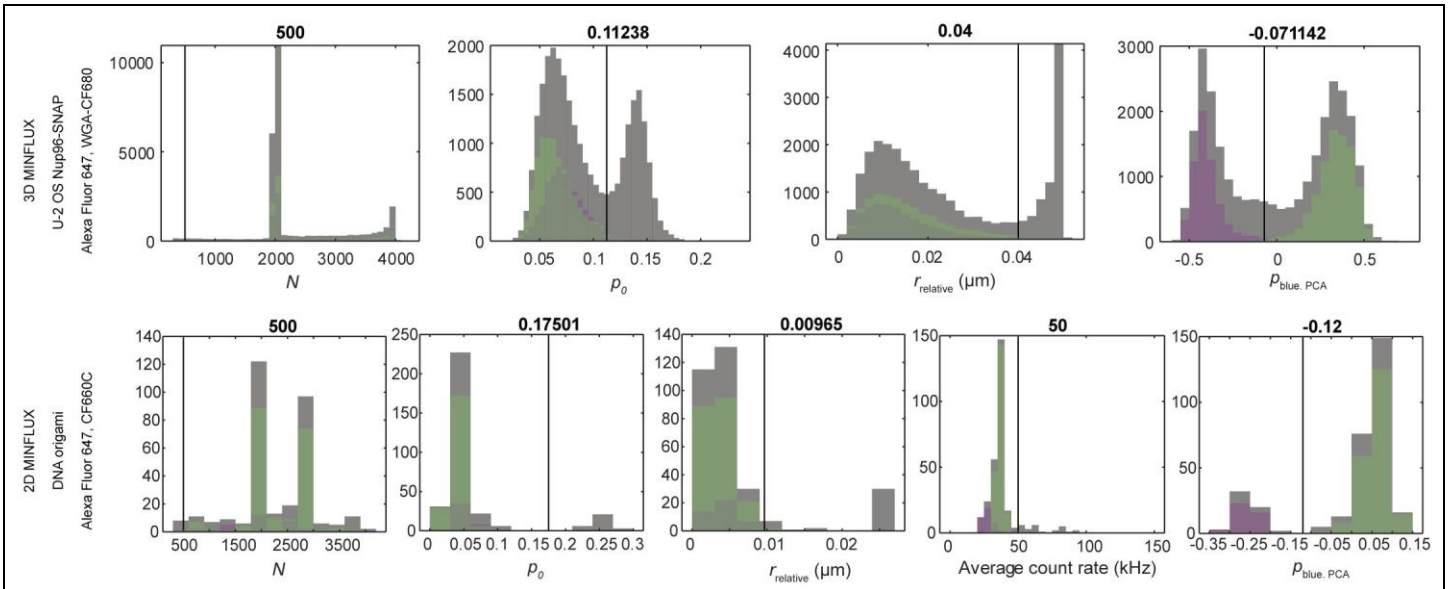

Supplementary Figure 9

Filtering of multicolor imaging data.

The histogram of photon number *N*, the relative photon count number in the central exposure p_0 and distance of the estimated position relative to the center of the last excitation beam pattern $r_{relative}$ are displayed for each localization. Before filtering (gray) at a manually defined position (black line, number above), p_0 and $r_{relative}$ show two populations. The population that is assigned to background events is discarded, leading to a new filtered distribution for each molecule species (green: Alexa Fluor 647, magenta: CF dye). Top row: data displayed in Fig. 5e. Bottom row: data displayed in Fig. 5c.

Supplementary tables

Tab. S1 | Variables and functions in the MINFLUX FPGA pseudo code. The following variables and functions are present in the pseudo code presented in fig. S2.

External variables

`scan_dwell_time`	Time to spend at each scan position.
`wait_abort`	Stop waiting for a molecule to appear.
`molec_threshold`	Count rate threshold for deciding whether there is a molecule present or not.
`act_dwell_time`	Time the activation beam is enabled.
`N`	Vector containing the target number of photons for each iteration.
`T`	Vector containing the max dwell time of each iteration.
`last_iteration`	Total number of iterations.

Internal variables

`scan_elapsed_time`	Elapsed time at the current scan position.
`scan_idx`	Index for the position of the long range scanner. In this implementation, the tip-tilt mirror.
`iter_idx`	Current iteration.
`multiplex`	Object containing the properties and methods for the MINFLUX excitation multiplexing. **`.beam_offset`**: offset added to all MINFLUX beam positions. It is meant to account the molecule localization of each intermediate iteration. **`.waiting_time`**: time to wait for the MINFLUX scanner to stabilize. **`.exposure_time`**: time the excitation beam. **`.beam_pos`**: vector with beam positions for all exposures.
`count_rate`	Low-pass-filtered fluorescence photon count rate. Available to check the presence of a molecule.
`mol_pos_abs(iter_idx)`	Location of the molecule at iteration iter_idx, with respect to the frame of reference of the beam scanner.
`mol_pos(iter_idx)`	Location of the molecule at iteration iter_idx, with respect to the reference frame of that iteration (meaning, with the origin at multiplex.beam_offet for that iteration).
`photon_count`	Accumulated photons in current iteration.
`elapsed_time`	Elapsed time since the iteration started.

Methods

`scanner.send(scan_pos)`	Function to retrieve the scanner coordinates from an internal FPGA memory (`scanner_positions`) and output them on the FPGA analog outputs.
	
	`scanner.send(scan_pos)`
	`  scan_pos = scanner_positions(scan_idx)`
	`  ao_scanner = scan_pos`
	`end`

`activation_beam.enable(act_dwell_time)`	Enable activation beam for a given dwell time.
`multiplex.load_settings(iter_idx)`	Loads the beam locations and dwell times that correspond to the iterations `iter_idx`
`multiplex.single_cycle()`	Send one MINFLUX exposure cycle. This means collecting a single instance of the photons counts `n0,n1,…` for each beam position `r0,r1,…`

`multiplex.start()` `multiplex.stop()`	Start and stop the continuous MINFLUX multiplexing, while accumulating the photon counts `n0,n1,…` and the beam positions `r0,r1,….`
`localize(iter_idx,n0,n1,n2,...)`	Localize the emitting molecule based on the collected photons and the knowledge of the beam distribution at iteration `iter_idx`.

Tab. S2 | Iterative MINFLUX strategies. Beam shapes as introduced in Fig. 1 and Fig. 3: G - regularly focused beam with 4 TCP positions at $x/y = \pm L/2$; D - 2D donut with 4 TCP positions in a triangle plus central position; Z - 3D donut with 2 TCP positions at $z = \pm L/2$; D7: 3D donut with 7 TCP positions at $x/y/z = \pm L/2$ plus central position.

		Beam shape	L (nm)	N_k	Estimator scaling factor	Estimator β_0	Estimator β_1
2D iterative MINFLUX imaging							
Simulations	Fig. 1	*G*	300	150	0.8	Optimal	
		D	150	100			
		D	90	120			
		D	40	230			
U-2 OS-NUP96-SNAP-AlexaFluor647 (2D)	Fig. 2a	*G*	300	100	0.8	-	-
		G	300	100	0.8	-	-
		D	150	150		0.89	7.18
		D	100	300		0.57	10.8
		D	50	10000		0.57	10.8
U-2 OS-NUP96-mMaple, live (2D)	Fig. 2f	G	300	100	0.8	-	-
		G	300	100	0.8	-	-
		D	150	150		0.099	6.1
		D	100	300		0.77	8.7
		D	100	10000		0.77	8.7
3D iterative MINFLUX imaging							
Simulations	Fig 3	*G*	300	150	0.8	Optimal	
		Z	400	100			
		D7	150	150			
		D7	90	150			
		D7	40	450			
U-2 OS-NUP96-SNAP-AlexaFluor647 (3D)	Fig. 3f	*G*	300	100	0.8	-	-
		G	300	100	0.8	-	-
		Z	300	100		0.55	-
		Z	200	100		0.55	-
		D7	150	150		0.88	23.5
		D7	100	200		0.58	31.5
		D7	100	10000		0.58	31.3
HPN-PSD95-HaloTag-AlexaFluor647 (3D)	Fig. 4a	*G*	300	100	0.8	-	-
		G	300	100	0.8	-	-
		Z	300	100		0.55	-
		Z	200	100		0.55	-
		D7	150	150		0.88	23.5
		D7	100	200		0.58	31.5
		D7	100	10000		0.58	31.3
Multicolor MINFLUX imaging							
U-2 OS-NUP96-SNAP-AlexaFluor647, WGA CF680 (3D)	Fig. 5e	*G*	300	100	0.8	-	-
		G	300	100	0.8	-	-
		Z	300	100		0.55	-
		Z	200	100		0.55	-
		D7	150	150		0.88	23.5
		D7	100	200		0.58	31.5
		D7	100	10000		0.58	31.3
DNA origami, AlexaFluor647, CF660C (2D)	Fig. 5c	G	300	100	1	-	-
		G	300	100	1	-	-
		D	150	300		1.16	8
		D	100	400		0.95	8.8
		D	50	5000		0.58	11.6

Tab. S3 | DNA origami strands.

Biotinylated

Biotin conjugated to 5‘ end, HPLC purified

47	CTTTGAAAAGAACTGGCTCATTATTTAATAAA
54	CCGGAAACACACCACGGAATAAGTAAGACTCC
103	CGAGTAGAACTAATAGTAGTAGCAAACCCTCA
106	GGTATTAAGAACAAGAAAAATAATTAAAGCCA
173	CTTGCATGCATTAATGAATCGGCCCGCCAGGG
180	CGGAATTATTGAAAGGAATTGAGGTGAAAAAT

For Alexa Fluor 647 labeling sites

39	TTATTCCTGTAGTATATGGCAATGAAATTATGCTCCATGAGAGGCTTTGAGGACTAGGGAGTT
41	TTATTCCTGTAGTATATGGCAATGAAATTATGCGAAACATGCCACTACGAAGGCATGCGCCGA
111	TTATTCCTGTAGTATATGGCAATGAAATTATCAAAATTAAAGTACGGTGTCTGGAAGAGGTCA
113	TTATTCCTGTAGTATATGGCAATGAAATTATTCAATTCTTTTAGTTTGACCATTACCAGACCG
130	TTATTCCTGTAGTATATGGCAATGAAATTATGGTAGCTAGGATAAAAATTTTTAGTTAACATC

For CF660C labeling sites

58	ACTAGCGGCAACGGCCCAACTATCCATTTTTTTCAACTATAGGCTGGCTGACCTTGTATCAT
75	ACTAGCGGCAACGGCCCAACTATCCATTTTACTGGATAACGGAACAACATTATTACCTTATG
77	ACTAGCGGCAACGGCCCAACTATCCATTTTCCAAAATATAATGCAGATACATAAACACCAGA
94	ACTAGCGGCAACGGCCCAACTATCCATTTTTACCTTTAAGGTCTTTACCCTGACAAAGAAGT

Marker strands

Dye conjugated to 5‘ end, PAGE purified

Alexa Fluor 647	TAATTTCATTGCCATATACTACAGGAATAA
CF660C	AAATGGATAGTTGGGCCGTTGCCGCTAGT

Staple strands

2	ACGTTAGTAAATGAATTTTCTGTAAGCGGAGT
3	CGTAACGATCTAAAGTTTTGTCGTGAATTGCG
4	TGTAGCATTCCACAGACAGCCCTCATCTCCAA
5	TGAGTTTCGTCACCAGTACAAACTTAATTGTA
6	CAAGCCCAATAGGAACCCATGTACCGTAACAC
7	CTCAGAGCCACCACCCTCATTTTCCTATTATT
8	CCCTCAGAACCGCCACCCTCAGAACTGAGACT
9	TATCACCGTACTCAGGAGGTTTAGCGGGGTTT
11	GAGAATAGCTTTTGCGGGATCGTCGGGTAGCA
12	AATAATAAGGTCGCTGAGGCTTGCAAAGACTT
13	AAAAAAGGACAACCATCGCCCACGCGGGTAAA
14	TCGGTTTAGCTTGATACCGATAGTCCAACCTA
15	AATGCCCCGTAACAGTGCCCGTATGTGAATTT
16	CTGAAACAGGTAATAAGTTTTAACCCCTCAGA
17	CCTCAAGAATACATGGCTTTTGATAGAACCAC
18	TGCTCAGTCAGTCTCTGAATTTACCAGGAGGT
21	AAAGGCCGAAAGGAACAACTAAAGCTTTCCAG
22	ATATATTCTTTTTTCACGTTGAAAATAGTTAG
23	CAATGACACTCCAAAAGGAGCCTTACAACGCC
24	CTTAAACATCAGCTTGCTTTCGAGAAACAGTT
25	TGCCTTGACTGCCTATTTCGGAACAGGGATAG
26	AGTGTACTTGAAAGTATTAAGAGGCCGCCACC
27	TAAGCGTCGAAGGATTAGGATTAGTACCGCCA
28	GGAAAGCGACCAGGCGGATAAGTGAATAGGTG
29	ACGGCTACTTACTTAGCCGGAACGCTGACCAA
30	TTTCATGAAAATTGTGTCGAAATCTGTACAGA
31	ATACGTAAAAGTACAACGGAGATTTCATCAAG
32	AAACGAAATGACCCCCAGCGATTATTCATTAC
33	GAGCCGCCCCACCACCGGAACCGCCTAAAACA
34	GCCACCACTCTTTTCATAATCAAACCGTCACC
35	CACCAGAGTTCGGTCATAGCCCCCGCCAGCAA
36	TGAGGCAGGCGTCAGACTGTAGCGTAGCAAGG
39	**Modified > Alexa Fluor 647**
40	CGCCTGATGGAAGTTTCCATTAAACATAACCG
41	**Modified > Alexa Fluor 647**
42	CTCATCTTGAGGCAAAAGAATACACTCCCTCA

43	AACCAGAGACCCTCAGAACCGCCAGGGGTCAG
44	GTTTGCCACCTCAGAGCCGCCACCGATACAGG
45	TCGGCATTCCGCCGCCAGCATTGACGTTCCAG
46	TGCCTTTAGTCAGACGATTGGCCTGCCAGAAT
47	**Modified > Biotin**
48	CCAGGCGCTTAATCATTGTGAATTACAGGTAG
49	AGTAATCTTAAATTGGGCTTGAGAGAATACCA
50	CCAAATCACTTGCCCTGACGAGAACGCCAAAA
51	TTATTCATAGGGAAGGTAAATATTCATTCAGT
52	GACTTGAGAGACAAAAGGGCGACAAGTTACCA
53	AATCACCAAATAGAAAATTCATATATAACGGA
54	**Modified > Biotin**
57	CGATTTTAGAGGACAGATGAACGGCGCGACCT
58	**Modified > CF660C**
59	ACGAGTAGTGACAAGAACCGGATATACCAAGC
60	GAATAAGGACGTAACAAAGCTGCTGACGGAAA
61	ATTGAGGGTAAAGGTGAATTATCAATCACCGG
62	AGCGCCAACCATTTGGGAATTAGATTATTAGC
63	TCACAATCGTAGCACCATTACCATCGTTTTCA
64	ACGCAAAGGTCACCAATGAAACCAATCAAGTT
65	ACGAACTAGCGTCCAATACTGCGGAATGCTTT
66	AAAGATTCAGGGGGTAATAGTAAACCATAAAT
67	CATTCAACGCGAGAGGCTTTTGCATATTATAG
68	GGAATTACTCGTTTACCAGACGACAAAAGATT
69	AAAAGTAATATCTTACCGAAGCCCAACACTAT
70	GAAGGAAAATAAGAGCAAGAAACAACAGCCAT
71	ATACCCAAGATAACCCACAAGAATAAACGATT
72	TTATTACGGTCAGAGGGTAATTGAATAGCAGC
75	**Modified > CF660C**
76	TTTGCCAGATCAGTTGAGATTTAGTGGTTTAA
77	**Modified > CF660C**
78	CATAACCCGAGGCATAGTAAGAGCTTTTTAAG
79	GCAATAGCGCAGATAGCCGAACAATTCAACCG
80	GCCCAATACCGAGGAAACGCAATAGGTTTACC
81	ATCAGAGAAAGAACTGGCATGATTTTATTTTG
82	TGAACAAACAGTATGTTAGCAAACTAAAAGAA
83	AAACAGTTGATGGCTTAGAGCTTATTTAAATA
84	CAAAAATCATTGCTCCTTTTGATAAGTTTCAT
85	TCAGAAGCCTCCAACAGGTCAGGATCTGCGAA
86	AAGAGGAACGAGCTTCAAAGCGAAGATACATT
87	CCTAATTTACGCTAACGAGCGTCTATATCGCG
88	ATTATTTAACCCAGCTACAATTTTCAAGAACG

89	TTTTGTTTAAGCCTTAAATCAAGAATCGAGAA
90	CTTTACAGTTAGCGAACCTCCCGACGTAGGAA
93	TTTTTGCGCAGAAAACGAGAATGAATGTTTAG
94	**Modified > CF660C**
95	GAAGCAAAAAAGCGGATTGCATCAGATAAAAA
96	TTTTAATTGCCCGAAAGACTTCAATTCCAGAG
97	TCTTACCAGCCAGTTACAAAATAAATGAAATA
98	TATTTTGCTCCCAATCCAAATAAGTGAGTTAA
99	AGGTTTTGAACGTCAAAAATGAAAGCGCTAAT
100	GAGGCGTTAGAGAATAACATAAAAGAACACCC
101	TGCAACTAAGCAATAAAGCCTCAGTTATGACC
102	TCCATATACATACAGGCAAGGCAACTTTATTT
103	**Modified > Biotin**
104	TCGCAAATGGGGCGCGAGCTGAAATAATGTGT
105	ATCGGCTGCGAGCATGTAGAAACCAGCTATAT
106	**Modified > Biotin**
107	CAAGCAAGACGCGCCTGTTTATCAAGAATCGC
108	TCATTACCCGACAATAAACAACATATTTAGGC
109	TATAGAAGCGACAAAAGGTAAAGTAGAGAATA
110	GCTAAATCCTGTAGCTCAACATGTATTGCTGA
111	**Modified > Alexa Fluor 647**
112	CAATAAATACAGTTGATTCCCAATTTAGAGAG
113	**Modified > Alexa Fluor 647**
114	TTTCATTTGGTCAATAACCTGTTTAATCAATA
115	CTAATTTATCTTTCCTTATCATTCATCCTGAA
116	TAAGTCCTACCAAGTACCGCACTCTTAGTTGC
117	AATGCAGACCGTTTTTATTTTCATCTTGCGGG
118	CCAGACGAGCGCCCAATAGCAAGCAAGAACGC
119	CTGTAATATTGCCTGAGAGTCTGGAAAACTAG
120	CAACGCAATTTTTGAGAGATCTACTGATAATC
121	TATATTTTAGCTGATAAATTAATGTTGTATAA
122	AGGTAAAGAAATCACCATCAATATAATATTTT
123	GCGTTATAGAAAAAGCCTGTTTAGAAGGCCGG
124	ACGCTCAAAATAAGAATAAACACCGTGAATTT
125	CATATTTAGAAATACCGACCGTGTTACCTTTT
126	AGAGGCATAATTTCATCTTCTGACTATAACTA
129	TCAGGTCACTTTTGCGGGAGAAGCAGAATTAG
130	**Modified > Alexa Fluor 647**
131	ACCGTTCTAAATGCAATGCCTGAGAGGTGGCA
132	AGACAGTCATTCAAAAGGGTGAGATATCATAT
133	AATTACTACAAATTCTTACCAGTAATCCCATC
134	AGGCGTTACAGTAGGGCTTAATTGACAATAGA

135	AATGGTTTACAACGCCAACATGTAGTTCAGCT
136	TTTTAGTTTTTCGAGCCAGTAATAAATTCTGT
137	CATGTCAAGATTCTCCGTGGGAACCGTTGGTG
138	AGAAAAGCAACATTAAATGTGAGCATCTGCCA
139	GCAAATATCGCGTCTGGCCTTCCTGGCCTCAG
140	GTTAAAATTTTAACCAATAGGAACCCGGCACC
141	TTAAGACGTTGAAAACATAGCGATTTAAATCA
142	ATCAAAATCGTCGCTATTAATTAACGGATTCG
143	TAACCTCCATATGTGAGTGAATAAACAAAATC
144	TATGTAAACCTTTTTTAATGGAAAAATTACCT
147	ACCCGTCGTCATATGTACCCCGGTAAAGGCTA
148	CTTTCATCCCCAAAAACAGGAAGACCGGAGAG
149	AAATAATTTTAAATTGTAAACGTTGATATTCA
150	GCTCATTTTCGCATTAAATTTTTGAGCTTAGA
151	TAGAATCCCTGAGAAGAGTCAATAGGAATCAT
152	CTGTAAATCATAGGTCTGAGAGACGATAAATA
153	AAATCAATGGCTTAGGTTGGGTTACTAAATTT
154	TTGAATTATGCTGATGCAAATCCACAAATATA
155	TAGATGGGGGGTAACGCCAGGGTTGTGCCAAG
156	GTTTGAGGGAAAGGGGGATGTGCTAGAGGATC
157	GAAGATCGGTGCGGGCCTCTTCGCAATCATGG
158	GCTTCTGGTCAGGCTGCGCAACTGTGTTATCC
159	CTTTTACACAGATGAATATACAGTAAGCGCCA
160	CCTGATTGAAAGAAATTGCGTAGACCCGAACG
161	GCGCAGAGATATCAAAATTATTTGACATTATC
162	GAGCAAAAACTTCTGAATAATGGAAGAAGGAG
165	ATTAAGTTCGCATCGTAACCGTGCGAGTAACA
166	CAGCTGGCGGACGACGACAGTATCGTAGCCAG
167	GGCGATCGCACTCCAGCCAGCTTTGCCATCAA
168	TTCGCCATTGCCGGAAACCAGGCAAACAGTAC
169	TTTAACGTTCGGGAGAAACAATAATTTTCCCT
170	ACAGAAATCTTTGAATACCAAGTTCCTTGCTT
171	AACCTACCGCGAATTATTCATTTCCAGTACAT
172	TGGATTATGAAGATGATGAAACAAAATTTCAT
173	**Modified > Biotin**
174	CCCGGGTACTTTCCAGTCGGGAAACGGGCAAC
175	TCATAGCTACTCACATTAATTGCGCCCTGAGA
176	GCTCACAATGTAAAGCCTGGGGTGGGTTTGCC

177	CGACAACTAAGTATTAGACTTTACAGCCGGAA
178	TTATTAATGCCGTCAATAGATAATCAGAGGTG
179	ATTTTGCGTCTTTAGGAGCACTAAGCAACAGT
180	**Modified > Biotin**
183	GCCAGCTGCCTGCAGGTCGACTCTGCAAGGCG
184	ACTGCCCGCCGAGCTCGAATTCGTTATTACGC
185	GTGAGCTAGTTTCCTGTGTGAAATTTGGGAAG
186	GCATAAAGTTCCACACAACATACGAAACAATT
187	GGATTTAGCGTATTAAATCCTTTGTTTTCAGG
188	AGATTAGATTTAAAAGTTTGAGTACACGTAAA
189	CTAAAATAGAACAAAGAAACCACCAGGGTTAG
190	ATCAACAGTCATCATATTCCTGATTGATTGTT
191	TGGTTTTTAACGTCAAAGGGCGAAGAACCATC
192	AGCTGATTACAAGAGTCCACTATTGAGGTGCC
193	GAGTTGCACGAGATAGGGTTGAGTAAGGGAGC
194	CCAGCAGGGGCAAAATCCCTTATAAAGCCGGC
195	ACGAACCAAAACATCGCCATTAAATGGTGGTT
196	AGGCGGTCATTAGTCTTTAATGCGCAATATTA
197	GCCACGCTATACGTGGCACAGACAACGCTCAT
198	CTAAAGCAAGATAGAACCCTTCTGAATCGTCT
201	TGGACTCCCTTTTCACCAGTGAGACCTGTCGT
202	AGTTTGGAGCCCTTCACCGCCTGGTTGCGCTC
203	GAATAGCCGCAAGCGGTCCACGCTCCTAATGA
204	CCGAAATCCGAAAATCCTGTTTGAAATACCGA
205	TAGCCCTACCAGCAGAAGATAAAAACATTTGA
206	GAATGGCTAGTATTAACACCGCCTCAACTAAT
207	GCGTAAGAGAGAGCCAGCAGCAAAAAGGTTAT
208	GCCAACAGTCACCTTGCTGAACCTGTTGGCAA
210	ACCCAAATCAAGTTTTTTGGGGTCAAAGAACG
211	GTAAAGCACTAAATCGGAACCCTAGTTGTTCC
212	CCCCGATTTAGAGCTTGACGGGGAAATCAAAA
213	GAACGTGGCGAGAAAGGAAGGGAACAAACTAT
214	CGGCCTTGCTGGTAATATCCAGAACGAACTGA
215	CCGCCAGCCATTGCAACAGGAAAAATATTTTT
216	GGAAATACCTACATTTTGACGCTCACCTGAAA
217	GAAATGGATTATTTACATTGGCAGACATTCTG

Supplementary notes

Wavelength dependence in MINFLUX

Localization by MINFLUX operates by placing the zero of an excitation intensity distribution proximal to the fluorophore to be localized. The curvature of the intensity profile depends on the intensity magnitude I_0 and the wavelength λ of the excitation light, which is why one may be induced to believe that these parameters significantly affect the MINFLUX localization precision. However, this is not the case, because this dependence vanishes under ideal conditions, and for realistic scenarios, the dependence has a high order. In this section, we will analyze several MINFLUX localization scenarios and their relation to the excitation wavelength.

(i) Quadratic beams with no background

The spatial dependence of the fluorescence emission around the intensity zero of a donut or a sine-shaped excitation beam, and hence also the mean of the detected photon number, can be approximated by: $n_i(x) = a(x - x_i)^2$. The curvature parameter a contains the intensity magnitude and the wavelength generally as $a = \alpha I_0/\lambda^2$, with α denoting a constant containing collection efficiency c_e, quantum efficiency q_e, absorption cross-section σ_A, dipole orientation κ and exposure time Δt.

As described before[1], the parameter vector $\vec{p}$ (equation S4) describing the success probabilities of a multinomial distribution for K exposures (equation S3) is given by

$$p_i = \frac{I_i}{\sum_{j=0}^{K-1} I_j} = \frac{a(x - x_i)^2}{\sum_{j=0}^{K-1} a\left(x - x_j\right)^2}$$

Any forthcoming statistical calculation will depend on $\vec{p}$, which has no dependence on the curvature, and therefore neither on the wavelength nor on the magnitude.

(ii) 1D MINFLUX with quadratic beams and background

When there is background or an imperfect zero of intensity, the detected fluorescence photon distribution is modified with a constant c added: $n_i(x) = a(x - x_i)^2 + c = a[(x - x_i)^2 + c\lambda^2/(\alpha I_0)]$. In this case, the parameter vector $\vec{p}$ keeps the wavelength dependence, and the Cramér-Rao bound at the origin for the 1D MINFLUX localization with two exposures (zeros separated a distance L) is

$$\sigma_{CRB}(x = 0) = \frac{1}{4}\frac{L}{\sqrt{N}}\left[1 + \frac{c\lambda^2/\alpha I_0}{\left(\frac{L}{2}\right)^2}\right]$$

The effect of the wavelength can be neglected as long as $c\lambda^2/\alpha I_0 \ll (L/2)^2$. When this is not possible, it gives rise to an optimal zero separation L, which was studied in [2].

In contrast to standard camera-based localization, where the CRB is directly proportional to the emission wavelength, the excitation wavelength dependence in MINFLUX is due to a non-vanishing (background and/or zero imperfection) signal contribution and scales with $(1 + \text{const}\,\lambda^2)$.

(iii) 2D MINFLUX with realistic beams and no background

If the realistic excitation beam shape is taken under consideration (instead of a quadratic approximation), a wavelength dependence appears within the shape of the beam. This is the case

for 2D MINFLUX with four exposures, as deduced before[1] (equation S30, background neglected), where for a beam defined as

$$I_{\mathrm{donut}}(\bar{r}) = A_0 4\mathrm{e}\ln 2\frac{r^2}{\mathrm{FWHM}^2}\mathrm{e}^{-4\ln 2\frac{r^2}{\mathrm{FWHM}^2}}$$

the CRB for MINFLUX is

$$\sigma_{\mathrm{CRB}}(x=y=0) = \frac{L}{2\sqrt{2N}}\left(1-\frac{L^2\ln(2)}{\mathrm{FWHM}^2}\right)^{-1}$$

The beam parameter FWHM is proportional to the wavelength, and for $L <$ FWHM the CRB can be approximated to $\sigma_{\mathrm{CRB}}(x=y=0) \approx (1+L^2\ln 2/\mathrm{FWHM}^2)\,L/\left(2\sqrt{2N}\right)$.

Due to the realistic shape of the beam, the wavelength dependence is of the form $(1+const\ \lambda^{-2})$. Hence, the longer the wavelength is, the better the precision will be, because the quadratic approximation is better fulfilled.

(iv) 2D MINFLUX with realistic beams and background

The case where all elements are joined (realistic beam shape and imperfect zero/background) was also studied in [1] including a signal-to-background parameter SBR. For that case, the dependence of the CRB is

$$\tilde{\sigma}_{CRB}(\bar{r}=\bar{0}) = \frac{L}{2\sqrt{2N}}\left(1-\frac{L^2\ln(2)}{FWHM^2}\right)^{-1}\sqrt{\left(1+\frac{1}{SBR(\bar{0})}\right)\left(1+\frac{3}{4\,SBR(\bar{0})}\right)}$$

where the SBR parameter is

$$SBR(\bar{r}_m) = \frac{\sum_{j=0}^{K-1}\lambda_j}{\sum_{j=0}^{K-1}\lambda_{bj}} \approx \frac{\mathrm{c_e}q_e\sigma_a\sum_{j=0}^{K-1}I_j(\bar{r}_m)}{\sum_{j=0}^{K-1}\lambda_{bj}}$$

In simple terms, the SBR is proportional to the curvature a, therefore $SBR \propto \lambda^{-2}$. The SBR dependence in the CRB can be approximated to $\approx 1+7/(8SBR)$.

As deduced for the 1D case, the 2D MINFLUX localization with realistic beams also holds a second order wavelength dependence $\propto 1+\mathrm{const}\,\lambda^2$, due to background and zero imperfection.

In conclusion, under ideal conditions MINFLUX localization holds no wavelength dependence. However, realistic experimental scenarios do hold a higher order dependence. Nevertheless, we stress that the real limitations are not coming from this spurious wavelength dependence, but from background and beam imperfections, most notably non-zero intensity minima, which may themselves be wavelength dependent.

References

1. Balzarotti, F. et al. Nanometer resolution imaging and tracking of fluorescent molecules with minimal photon fluxes. Science 355, 606-612 (2017).
2. Eilers, Y., Ta, H., Gwosch, K.C., Balzarotti, F. & Hell, S.W. MINFLUX monitors rapid molecular jumps with superior spatiotemporal resolution. *Proc. Natl. Acad. Sci. U.S.A.* **115**, 6117-6122 (2018).